Applied Physics Letters ARTICLE scitation.org/journal/apl

Experimental demonstration of energy harvesting from the sky using the negative illumination effect of a semiconductor photodiode

Cite as: Appl. Phys. Lett. **114**, 161102 (2019); doi: 10.1063/1.5089783
Submitted: 22 January 2019 · Accepted: 17 March 2019 ·
Published Online: 23 April 2019

Masashi Ono,[1,2] Parthiban Santhanam,[1] Wei Li,[1] Bo Zhao,[1] and Shanhui Fan[1,a)]

AFFILIATIONS

[1]Ginzton Laboratory, Department of Electrical Engineering, Stanford University, Stanford, California 94305, USA
[2]Fujifilm Corporation, Frontier Core-Technology Laboratories, 577 Ushijima, Kaisei-machi, Ashigarakami-gun, Kanagawa 258-8577, Japan

[a)]shanhui@stanford.edu

ABSTRACT

We experimentally demonstrate electric power generation from the coldness of the universe directly, using the negative illumination effect when an infrared semiconductor diode faces the sky. Our theoretical model, accounting for the experimental results, indicates that the performance of such a power generation scheme is strongly influenced by the degree of matching between the responsivity spectrum and the atmospheric transparency window, as well as the quantum efficiency of the diode. A Shockley-Queisser analysis of an ideal optimized diode, taking into consideration the realistic transmissivity spectrum of the atmosphere, indicates the theoretical maximum power density of 3.99 W/m^2 with the diode temperature at 293 K. The results here point to a pathway towards night-time power generation.

It was recently noted theoretically and demonstrated experimentally that a semiconductor photodiode, undergoing radiative exchange with a colder surface, can generate power by harvesting the outgoing thermal radiation from the diode.[1–5] This negative illumination effect is in contrast with an usual "positive illumination" mode of operation for energy harvesting, such as the operation of a solar cell, where the photodiode harvests incoming thermal radiation from a hotter surface.

Since the sky has a temperature colder than the temperature of the earth surface, one should be able to use the negative illumination effect to harvest the outgoing thermal radiation from the earth surface, by having a semiconductor photo-diode facing the sky. The theoretical limits for the achievable power density in such a scheme have been computed for a diode directly facing a surface at a temperature of 3 K, which corresponds to the temperature of outer space, but without taking into account the effect of the atmosphere.[1,3] Neither have there been any experimental demonstration of the use of the negative illumination effect on the earth to directly harvest power from outgoing thermal radiation.

In this letter, we provide an experimental demonstration of energy harvesting of outgoing thermal radiation from the earth surface to the sky through negative illumination. We account for the experimental results with a theoretical model that takes into account both the transmission of the sky and the nonideality of the diode. Using this model, we show that given the transmission coefficient of the sky in our experiment, an ideal diode can extract a power density of 3.99 W/m^2.

The sky has an atmospheric transparency window ranging from 8 to 13 μm, where the transmissivity of the sky is high. Thermally emitted photons from the earth's surface in this wavelength range can escape to outer space. Such a transparency window thus enables one to have access to the coldness of the outerspace, which is the basis for all radiative cooling experiments.[6–17] For our purposes here, in order to use the negative illumination effect for energy harvesting from the sky, it is important that the diode has significant above-bandgap emissivity in the transparency window.

In our experiment, we therefore choose to use an infrared HgCdTe photodiode (Vigo's PV-4TE-10.6). The experimental setup is shown in Fig. 1(a). The photodiode undergoes radiative exchange with clear sky through a 90° off-axis parabolic mirror, which has a focal length of 2-in. The parabolic mirror restricts the photon flux to the diode to only those coming from the sky. An optical chopper, with its blades rotating at a frequency of 407 Hz, is placed between the diode and the parabolic mirror to carry out the lock-in measurement. The

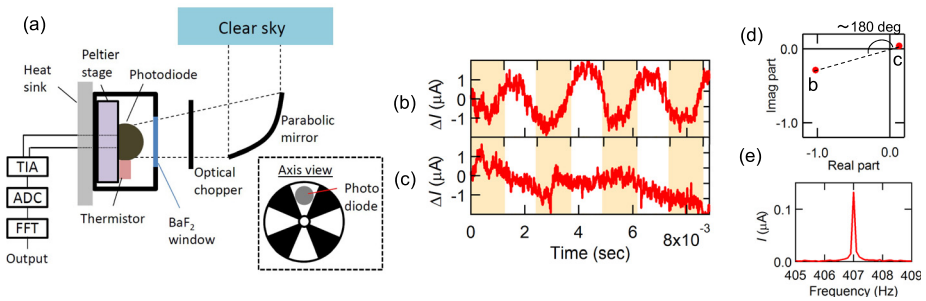

FIG. 1. (a) Schematic diagram of the experimental setup. (b) and (c) Time-domain photocurrent data in the case where the diode is at an ambient temperature of 293 K. The diode faces a radiative surface at a temperature of 343 K (b) and the sky (c), respectively. All photocurrent data in (b) and (c) are offset by the first data point. (d) The complex amplitude of the Fourier components in (b) and (c) at the frequency of the chopper. (e) The photocurrent spectrum, for the case in (c), when the diode is at the ambient temperature of 293 K and faces the sky.

chopper has a 50–50 duty cycle. The diode is covered by a hemispherical GaAs immersion lens and has a 35° field of view (FOV). A thermistor and a Peltier stage are used to simultaneously control and monitor the diode temperature.

In the measurement, the time-dependent photocurrent is amplified with 10^5 V/A transimpedance gain and read out by an analog-to-digital converter at a sampling rate of 10^5 Hz for a duration of 10 s. Subsequently, the time-dependent data are processed using a Fast Fourier Transform (FFT). This setup and the signal processing algorithms are similar to those in Ref. 1, where a negative illumination effect was observed in an indoor experiment. The main differences here are the sky access and the choice of the photodiode that enables power harvesting from the sky.

Figures 1(b) and 1(c) show the raw time-dependent photocurrent data obtained in the case where the diode is maintained at an ambient temperature of 293 K. Here, we estimated an ambient temperature of 293 K from the thermistor resistance attached to the photodiode. We did these experiments when the temperature of the diode and the ambient temperature were identical. In the analysis below, we assume that the heat needed to maintain the diode temperature is either supplied from the earth by conduction or from the ambient air by convection.

Figure 1(b) shows the case where the diode faces a surface hotter than the diode with a temperature of 343 K, and Fig. 1(c) shows the case where the diode faces the sky. The photocurrent oscillates due to the rotation of the chopper blade. As was noted in Ref. 1, the sign of the photocurrent generated by the photodiode changes between the positive and negative illumination cases. Therefore, one should expect a 180° phase change in the temporal oscillation of the photo-current between the positive and negative illumination cases. In Fig. 1(d), we plot the complex Fourier component of the photo-current at the chopper frequency and indeed observe the 180° phase difference between the positive [Fig. 1(b)] and negative illumination cases [Fig. 1(c)]. In the case where the photodiode is maintained at the ambient temperature and facing the sky, the oscillation of the photocurrent at the chopper frequency is not immediately visible as shown in Fig. 1(c). Nevertheless, the Fourier transform of the time-dependent photocurrent clearly shows a peak at the chopper frequency [Fig. 1(e)] with a signal to noise ratio exceeding 10^2. The use of the chopper here enables us to provide an accurate measurement in the cases when the photocurrent is relatively weak.

Based on the lock-in measurement technique as described above, we observe that the diode generates a current of 0.148 μA when it faces the sky. The maximum extractable power P_m is calculated as

$$P_m = \frac{1}{4} I_{sc}^2 R_{ZB}. \quad (1)$$

In Eq. (1), I_{sc} is the short circuit current. Our measured current corresponds to the short circuit current. In the negative illumination scenario, the I–V curve shifts up as compared to that in the equilibrium case.[1] In our experiment, since the power generated is small, the shift-up of the I–V curve is small. Also, the photodiode used in this work is nearly linear around 0 V. We therefore assume the resistance of the diode to be that at zero-bias, R_{ZB}. For our diode, R_{ZB} is measured at 11.7 kΩ with the diode temperature at 293 K. Using Eq. (1), the maximum extractable power under negative illumination is determined to be 6.39×10^{-2} μW/m^2 in the current experimental condition. The efficiency of power generation, as estimated from the ratio of the experimentally obtained power to outgoing heat flux, is 2.3×10^{-5}%, where the outgoing heat flux is calculated by the detailed-balance model,[18] taking into account the cutoff wavelength of 8.27 μm at room temperature and the transmissivity of the atmosphere. Such a low power density and efficiency come from the imperfect match between the emissivity of the diode and the transmissivity of the atmosphere and nonradiative recombination, as discussed later. Nevertheless, these results show that one can generate current under negative illumination, and hence electric power, with a photodiode directly facing the sky. Such a demonstration of direct power generation of a diode facing the sky has not been previously reported.

Below, we provide a detailed theoretical model that quantitatively accounts for the observed current when the diode is maintained at the ambient temperature and faces the sky. Moreover, in order to validate the model, we also experimentally measure the response of the diode in the same setup as in Fig. 1(a), but with its temperature different from the ambient temperature. We show that this model can account for the measured photocurrent over a wide range of diode temperatures. Our theoretical model highlights the important factors that control the performance of the device.

In our lock-in measurement, the observed signal I_{total}, i.e., the peak amplitude in the spectrum as shown in Fig. 1(e), corresponds to the *difference* between the photocurrent I_{sky} when the diode faces the sky, and the photocurrent I_{blade} when the diode faces the blade, i.e.,

$$I_{total} = I_{sky} - I_{blade}. \quad (2)$$

Here

$$I_{sky} = A\int R(\lambda, T_{diode})\{I_{BB}(\lambda, T_{diode}) - (1-\epsilon_{atm}(\lambda))I_{BB}(\lambda, T_{universe}) - \epsilon_{atm}(\lambda)I_{BB}(\lambda, T_{atm})\}d\lambda. \quad (3)$$

In Eq. (3), the first, second, and third terms in the braces are the outgoing photon flux from the diode, the incoming photon flux from universe, which is mostly in atmospheric transparency window (8–13 μm), and the incoming photon flux from the atmosphere, respectively. $R(\lambda, T_{diode})$ is the experimentally measured spectral responsivity at 293 K shown in Fig. 2(b). $I_{BB}(\lambda, T) = \left(2hc^2/\lambda^5\right)(\exp(hc/\lambda k_B T) - 1)^{-1}$ is the spectral radiance of a blackbody at temperature T, where h is Planck's constant, k_B is the Boltzmann constant, and c is the speed of light. T_{diode}, $T_{universe}$, and T_{atm} are the temperatures of the diode, the universe (3 K), and the atmosphere (298 K), respectively. The angle-dependent emissivity of the atmosphere is given by $\epsilon_{atm}(\theta, \lambda) = 1 - t(\lambda)^{1/\cos\theta}$, where $t(\lambda)$ is atmospheric transmittance in the zenith direction, obtained from MODTRAN5.[19] Since the diode has 35° FOV, and the I_{BB} (λ, T_{atm}) term does not have angle dependence, in Eq. (3) for ϵ_{atm}, we average ϵ_{atm} (θ) within a 35° solid angle. A is a constant with a dimension of area, which is used to account for the area of the diode, as well as other factors, e.g., how efficiently the diode interacts with the sky through the chopper blade and the parabolic mirror, how accurately the position of each optical devices is adjusted, and a factor used to convert the responsivity value obtained in arbitrary units by FTIR measurement to that in A/W. A is independent of the temperature of the diode. Here, for simplicity, we assumed that the responsivity of the diode is constant within 35° FOV, since the responsivity change associated with angle-averaged treatment is not significant and can be included to the geometrical factor A. In the temperature range we examined, the incoming photon flux from universe (second term) can be neglected, because the spectral irradiance from 3 K black body is extremely low. The radiative cooling effect then manifests in the *lack* of radiation from the atmosphere in the atmospheric transparency window.

When the diode faces the blade, its current is

$$I_{blade} = A\int R(\lambda, T_{diode})[I_{BB}(\lambda, T_{diode}) - I_{BB}(\lambda, T_{amb})]d\lambda. \quad (4)$$

Since the blade is a diffusive surface that has the same temperature as the ambient temperature T_{amb}, the blade emits thermal radiation at T_{amb} and simultaneously reflects thermal radiation at T_{amb}. Thus, the total radiation received by the diode from the blade is equal to the emission from a black body emitter at T_{amb}.

In Fig. 2(a), we compare the results from the theoretical model above to the experimental result. In the experiment, we use the same setup as shown in Fig. 1(a) and vary the diode temperature from below to above ambient temperature. The theoretical model, with a single fitting parameter of $A = 0.545\,mm^2$, as obtained by matching the theory with the experiment at the diode temperature $T_{diode} = 221$ K, agrees very nicely with the experimental results over the entire temperature range. The experiment data therefore validates the theoretical model. When the diode is at the ambient temperature of 293 K, $I_{blade} = 0$, and the measured total current only has contributions from the sky. The theoretical model predicts a photocurrent of 0.126 μA, which agrees reasonably well with the experimentally measured photocurrent of 0.148 μA as mentioned above.

The theoretical analysis, as outlined above, allows us to obtain the contributions from the sky and from the blade separately using Eqs. (3) and (4). In Fig. 2(a), we show I_{blade}(blue curve) and I_{sky}(red curve) as a function of the diode temperature. Here, we follow the usual sign convention of the PV cell: under positive(negative) illumination, the photocurrent has a negative(positive) value. We see that the blade contribution, I_{blade}, flips its sign from negative to positive at ambient temperature (293 K), as expected since the diode is maintained at the same ambient temperature. On the other hand, the sky contribution, I_{sky}, flips its sign at 288 K. Thus, in the current experimental condition, the sky has an effective temperature of 288 K or about 5 K below the ambient temperature. This effective temperature of the sky appears high, as compared to the value indicated by the previous radiative cooling work,[14] where cooling to 40 K below ambient air temperature has been demonstrated. In our experiment, the high effective temperature of the sky arises due to significant diode responsivity in the wavelength range outside the atmospheric transparency window, as shown in Fig. 2(b).

In Fig. 2(b), we also note that as the diode temperature reduces, the edge of the responsivity shifts from a cutoff wavelength of 8.27 μm at 293 K to a longer wavelength, which is attributed to the change in the Fermi level when the diode is cooled, known as the Moss-Burstein effect.[20,21] The responsivity spectra thus overlaps better with the transparency window. The magnitude of the responsivity is also

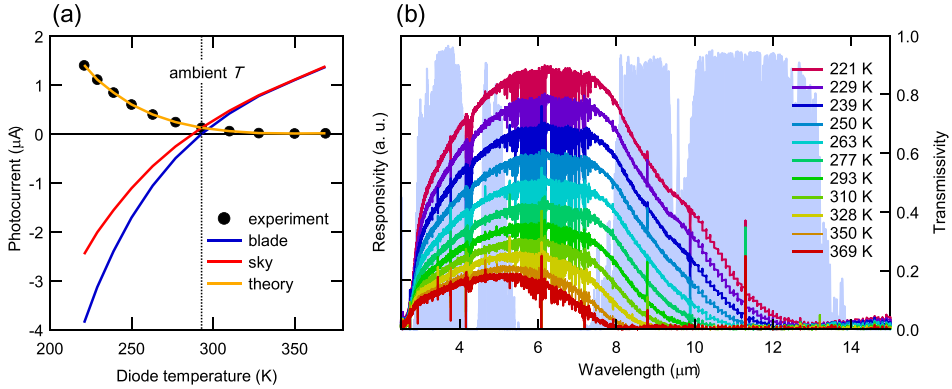

FIG. 2. (a) The total photocurrent amplitude (black dot), the photocurrent component contributed by the chopper blade (blue curve), the photocurrent component contributed by the sky (red curve), and theoretically calculated photocurrent trace (yellow curve), as a function of the diode temperature. The temperature of the diode is calculated from the thermistor resistance set onto the Peltier stage. (b) Temperature dependence of the spectral responsivity (left axis). Each color shows a diode temperature. The shaded region shows the transmissivity of the atmosphere (right axis).

significantly improved, which is due to suppression of detrimental effects such as Auger recombination and carrier scattering.[22–24] On the other hand, as the diode temperature goes down, the spectral radiance of the diode, i.e., the $I_{BB}(\lambda,\ T_{diode})$ term in Eq. (3), also decreases. Thus, when the diode temperature is below 288 K, the absorbed photon flux from downward atmospheric radiation still dominates over the outgoing radiative flux of the diode, and hence, the diode remains in the positive illumination regime.

In Fig. 3(a), we plot as the black curve the power density as a function of the diode temperature, when the diode is facing the sky. The power density is inferred using Eq. (1). The short circuit current I_{sc} is taken from the red curve in Fig. 2(a). We measure the zero-bias resistance of the diode, R_{ZB}, as a function of the diode temperature, as shown in Fig. 3(b). R_{ZB} changes from 13.41 Ω to 10.23 Ω as the diode temperature varies from 221 to 369 K. The power density shows a dip at a temperature of 288 K, corresponding to the effective temperature of the sky as discussed above. At a temperature above 288 K, the diode operates in the negative illumination regime, and the power density increases as a function of diode temperature. This is consistent with thermodynamic considerations: the power extraction here exploits the temperature difference between the diode itself and the sky. Increasing such a temperature difference is therefore favorable for power extraction. By increasing the diode temperature from 293 K to 369 K, the power density increases by about 80 times. This result points to the interesting possibility of using the sky-facing diode for low-grade waste heat recovery purposes.

Before we end this paper, we provide a comparison between our experimental results and a detailed-balance theoretical limit[18] of power extraction from the sky, taking into account the transmissivity spectrum of the sky. For this purpose, we assume a semiconductor with a bandgap at the angular frequency of ω_{Eg}. The semiconductor is assumed to have zero absorptivity below the bandgap and unity absorptivity above the bandgap. The generated power has the form

$$P = \frac{A_{optical} q V \eta}{4\pi^2 c^2}\left\{\int_{\omega_{Eg}}^{\infty} \frac{\omega^2 d\omega}{e^{\frac{\hbar\omega - qV}{k_B T_{diode}}} - 1} - \epsilon_{atm}\int_{\omega_{Eg}}^{\infty} \frac{\omega^2 d\omega}{e^{\frac{\hbar\omega}{k_B T_{atm}}} - 1}\right\}, \quad (5)$$

where $A_{optical}$ is the optical area of the diode, q is the elementary electric charge, V is the voltage of the diode, ω is the angular frequency, and η is the external quantum efficiency (EQE) of the diode. In Eq. (5), the first and second terms express the outgoing photon flux from the diode and the incoming photon flux from the atmosphere, respectively. The maximum extractable power is calculated by optimizing bandgap energy and applied voltage at each T_{diode} and is plotted in Fig. 3(a) (red curve). The power exhibits a dip at a temperature of 269 K, which is far lower than the experimentally observed effective sky temperature of 288 K, and indicates that our assumed spectrum here provides much better overlap with the transparency window of the atmosphere. When the diode is at the ambient temperature of 293 K, Eq. (5) predicts a maximum power density of 3.99 W/m^2 when the bandgap wavelength is at 13.2 μm. In the ideal condition, the efficiency of power generation estimated from the ratio of the power density to the outgoing heat flux is 10.2%. The detailed-balance analysis here thus points to significant room for improvement in the negative illumination concept. This value is still lower than that of the Shockley-Queisser limit in negative illumination [~54.8 W/m^2 (Refs. 1 and 3)], where the emissivity of the atmosphere is not considered. The relatively small value comes from thermal radiation from the atmosphere measured in the diode mainly in the wavelength range outside the transparency window. If we can reduce the responsivity in the wavelength range outside the transparency window while keeping η of 1, the achievable power output would approach the Shockley-Queisser limit of negative illumination. Assuming an η value of 0.14, the same as the diode we used in this research, the power density curve simply shifts to a lower level as compared to the result with $\eta = 1$, as shown in Fig. 3(a). This indicates that if the bandgap wavelength, the responsivity spectrum, and the applied bias are optimized, the power density can be significantly improved as compared to the current experimental condition even in the case where the EQE is not idealized.

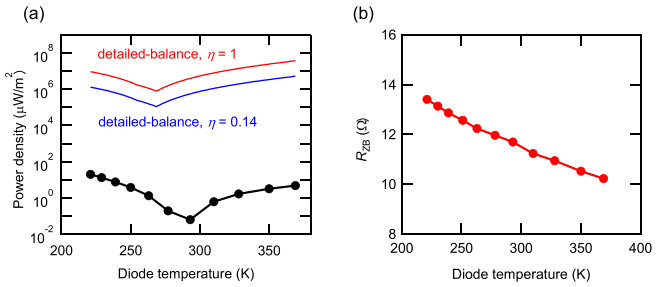

FIG. 3. (a) Calculated power density as a function of the diode temperature with the current experimental condition (black-dotted curve). The power densities calculated by the detailed-balance model with taking into account the emissivity of the atmosphere are shown by the red curve ($\eta = 1$) and the blue curve ($\eta = 0.14$). (b) Differential resistance R_{ZB} as a function of the diode temperature.

The analysis above shows that to improve the power generation from sky using negative illumination, it is necessary to reduce the Auger recombination and the concentration of majority carrier while maintaining the effective energy bandgap to be 0.094 eV, corresponding to a cutoff wavelength of 13.2 μm, for emitting outgoing photon flux via the atmospheric window. One method to achieve this is by employing low dimensional structures. It has been reported that quantum-confined structures, such as quantum wells or quantum dots, can be used to reduce the Auger recombination.[25,26] Furthermore, quantum dot structures have an advantage that their responsivity does not significantly depend on the diode temperatures.[27] These structures might be good candidates for achieving high responsivity even at ambient temperature for energy harvesting under negative illumination.

In conclusion, we have demonstrated power generation from the sky under negative illumination. We have also established a theoretical model that accounts for the observed temperature dependence of the photocurrent. The power density under outside negative illumination depends on the responsivity of the diode in and outside the atmospheric window as well as the quantum efficiency of the diode. Using a Shockley-Queisser analysis and taking into account the transmission spectrum of the atmosphere, we found that a maximum power of 3.99 W/m^2 can be achievable under negative illumination. Our results point to a pathway for energy harvesting during the night-time directly using the coldness of outer space.

This work was supported by the U.S. Department of Energy under Grant No. DE-FG02-07ER46426, by the U.S. Department of Energy "Photonics at Thermodynamic Limits" Energy Frontier Research Center under Grant No. DE-SC0019140, and by the U.S. National Science Foundation Grant No. CMMI-1562204.

REFERENCES

[1]P. Santhanam and S. Fan, "Thermal-to-electrical energy conversion by diodes under negative illumination," Phys. Rev. B **93**, 161410(R) (2016).
[2]S. J. Byrnes, R. Blanchard, and F. Capasso, "Harvesting renewable energy from Earth's mid-infrared emissions," Proc. Natl. Acad. Sci. U. S. A. **111**, 3927 (2014).
[3]S. Buddhiraju, P. Santhanam, and S. Fan, "Thermodynamic limits of energy harvesting outgoing thermal radiation," Proc. Natl. Acad. Sci. U. S. A. **115**, E3609 (2018).
[4]P. Berdahl, "Radiant refrigeration by semiconductor diodes," J. Appl. Phys. **58**, 1369–1374 (1985).
[5]W. C. Hsu, J. K. Tong, B. Liao, Y. Huang, S. V. Boriskina, and G. Chen, "Entropic and near-field improvements of thermoradiative cells," Sci. Rep. **6**, 34837 (2016).
[6]S. Catalanotti, V. Cuomo, G. Piro, D. Ruggi, V. Silverstrini, and G. Troise, "The radiative cooling of selective surfaces," Sol. Energy **17**, 83–89 (1975).
[7]P. Berdahl, M. Martin, and F. Sakkal, "Thermal performance of radiative cooling panels," Int. J. Heat Mass Transfer **26**, 871–880 (1983).
[8]A. R. Gentle and G. B. Smith, "Radiative heat pumping from the earth using surface phonon resonant nanoparticles," Nano Lett. **10**, 373–379 (2010).
[9]E. Rephaeli, A. Raman, and S. Fan, "Ultrabroadband photonic structures to achieve high-performance daytime radiative cooling," Nano Lett. **13**, 1457–1461 (2013).
[10]A. Raman, M. A. Anoma, L. Zhu, E. Rephaeli, and S. Fan, "Passive radiative cooling below ambient air temperature under direct sunlight," Nature **515**, 540–544 (2014).
[11]N. N. Shi, C.-C. Tsai, F. Camino, G. D. Bernard, N. Yu, and R. Wehner, "Keeping cool: Enhanced optical reflection and heat dissipation in silver ants," Science **349**, 298–301 (2015).
[12]A. R. Gentle and G. B. Smith, "A subambient open roof surface under the mid-summer sun," Adv. Sci. **2**, 1500119 (2015).
[13]M. M. Hossain, B. Jia, and M. Gu, "A metamaterial emitter for highly efficient radiative cooling," Adv. Opt. Mater. **3**, 1047–1051 (2015).
[14]Z. Chen, L. Zhu, A. Raman, and S. Fan, "Radiative cooling to deep sub-freezing temperatures through a 24-h day-night cycle," Nat. Commun. **7**, 13729 (2016).
[15]Y. Zhai, Y. Ma, S. N. David, D. Zhao, R. Lou, G. Tan, R. Yang, and X. Yin, "Scalable-manufactured randomized glass-polymer hybrid metamaterial for daytime radiative cooling," Science **355**, 1062–1066 (2017).
[16]J. I. Kou, Z. Jurado, Z. Chen, S. Fan, and A. Minnich, "Daytime radiative cooling using near-black infrared emitters," ACS Photonics **4**, 626–630 (2017).
[17]E. A. Goldstein, A. P. Raman, and S. Fan, "Sub-ambient non-evaporative fluid cooling with the sky," Nat. Energy **2**, 17143 (2017).
[18]W. Shockley and H. J. Queisser, "Detailed balance limit of efficiency of p-n junction solar cells," J. Appl, Phys. **32**, 510 (1961).
[19]A. Berk, G. P. Anderson, P. K. Acharya, L. S. Bernstein, L. Muratov, J. Lee, M. Fox, S. M. Adler-Golden, J. H. Chetwynd, Jr., M. L. Hoke, R. B. Lockwood, J. A. Gardner, T. W. Cooley, C. C. Borel, P. E. Lewis, and E. P. Shettle, "MODTRAN5: 2006 update," Proc. SPIE **6233**, 62331F (2006).
[20]D. H. Mao, A. J. Syllaios, H. G. Robinson, and C. R. Helms, "Optical absorption of un-implanted and implanted HgCdTe," J. Electron. Mater. **27**, 703–708 (1998).
[21]M. Z. I. Gering and K. B. White, "The Burstein-Moss shift for mercury cadmium telluride," J. Phys. C: Solid State Phys. **20**, 1137–1145 (1987).
[22]A. Rogalski, "HgCdTe infrared detector material: History, status and outlook," Rep. Prog. Phys. **68**, 2267–2336 (2005).
[23]P. Martyniuk and A. Rogalski, "Hot infrared photodetectors," Opto-Electron. Rev. **21**, 239–257 (2013).
[24]J. A. Gonzalez-Cuevas, T. F. Refaat, M. N. Abedin, and H. E. Elsayed-Ali, "Modeling of the temperature-dependent spectral response of $In_{1-x}Ga_xSb$ infrared photodetectors," Opt. Eng. **45**, 044001 (2006).
[25]L. C. Chiu and A. Yariv, "Auger recombination in quantum-well InGaAsP heterostructure lasers," IEEE J. Quantum Electron. **18**, 1406–1409 (1982).
[26]G. E. Cragg and A. L. Efros, "Suppression of Auger processes in confined structures," Nano Lett. **10**, 313–317 (2010).
[27]P. Bhattacharya, X. H. Su, S. Chakrabarti, G. Ariyawansa, and A. G. U. Perera, "Characteristics of a tunneling quantum-dot infrared photodetector operating at room temperature," Appl. Phys. Lett. **86**, 191106 (2005).